Chin. J. Astron. Astrophys. Vol. 7 (2007), No. 3, 405–414
(*http://www.chjaa.org*)

Chinese Journal of
Astronomy and
Astrophysics

The Chemical Composition of the Field Zero-Age Star HD 77407 *

Xue-Liang Zhu[1,2], Jian-Rong Shi[2], Gang Zhao[2], Ji Li[2,3] and Qing-Xiang Nie[1]

[1] College of Physics and Electronics, Shandong Normal University, Jinan 250014
[2] National Astronomical Observatories, Chinese Academy of Sciences, Beijing 100012; *gzhao@bao.ac.cn*
[3] Department of Physics, Hebei Normal University, Shijiazhuang 050016

Received 2006 December 8; accepted 2007 April 23

Abstract High-resolution optical spectra of the zero age star HD77407 are analysed and its Li, C, O, Na, Mg, Al, Si, K, Ca, Sc, Ti, V, Co, Ni and Ba contents are determined using spectral synthesis method. The temperature of the star is determined by fitting the H_α line wings. The parameters derived for this star are $T_{\rm eff}$=5900 K, $\log\ g$=4.47 and [Fe/H] = +0.07. It is found that the derived iron content is slightly higher than what is given in the published literature. This star shows a relative overabundances of Ca and Ba, and underabundances of Na, V and Ni with respect to the solar mix. Activity of the star is indicated by the filled in H_α and Ca II triplet line cores. It has been confirmed that our spectroscopic approach yields fairly reliable and consistent results for active stars.

Key words: stars: abundances — stars: ZAMS — stars: individual: HD77407

1 INTRODUCTION

The study of zero age main sequence (ZAMS) stars is usually focused on members of open clusters and associations. However, we can expect that ZAMS stars can also be found in the field, and particularly in the solar neighborhood. Such stars have following two properties: firstly, the lithium 6707.8 Å equivalent widths ($EW_{\rm Li}$) are in excess of the Pleiades upper limit of their respective spectral type; secondly, the X-ray activity of these stars is very high ($\log L_{\rm X}/L_{\rm bol}$ is about –3.49, Wichmann & Schmitt 2003). These two observational indicators suggest that the age of these stars is no more than about 50 Myr (Wielen 1977). Recently, ten such G-type field stars have been found in an extensive all-sky survey of nearby ZAMS stars in the solar neighborhood (Wichmann et al. 2003).

Young solar-type stars can be used as proxies for the early Sun, and they provide us with insight into its intense zero-age main sequence magnetic activity. It is noted that the surface X-ray activity of binaries does seem to be enhanced compared with single stars with the same rotation period (Güdel 2004), and the rotation is thought to be a necessary condition for magnetic activity. However, it is not clear as to what extent binarity influences the generation and morphology of magnetic field, and the corresponding chromospheric and coronal emission (Shkolnik et al. 2003). Furthermore, with improved instrumentation, more and more single stars turn out to have variable radial velocity (RV) due to the presence of low-mass companions, either low-mass stars, brown dwarfs or giant planets. It is thus becoming necessary and indeed possible to deal properly with the effects of binarity, and to attempt to separate the classical dynamo process of internal differential rotation from the external contribution from close companions (Dall et al. 2005).

One new area of investigation which has opened up since the advent of enhanced resolution X-ray spectroscopy is the study of the metal abundance in coronal plasmas. Abundance values significantly lower than the solar have been derived (Jordan et al. 1998). In the Sun it is known that the coronal abundances are not

* Supported by the National Natural Science Foundation of China.

the same as the photospheric ones, with the elements of lower first ionization potential (FIP) being enhanced (Young 2005). The individual coronal abundances of other stars are becoming available. A detailed comparison between coronal and photospheric abundances in active stars would provide useful insights into the chemical fractionation processes that are likely to operate between the photosphere and the corona. To study this issue, however, it is obviously necessary to have a detailed knowledge of the photospheric abundances of the stars under investigation. Unfortunately, such a comparison is made difficult by the extreme paucity of photospheric abundance determinations for elements other than iron. Another issue is the heterogeneous nature of the abundance analyses performed to date, often resulting in conflicting results in the literature. Despite the fact that active stars are known to exhibit photometric anomalies related to their high level of activity (Favata et al. 1997), most studies of the iron abundance in active stars have relied on temperatures derived from photometric indices (e.g., Randich et al. 1993). Therefore, the reliability of photometric colours as temperature indicators in active stars and the possible impact on the resulting abundances need to be investigated.

This paper is organized as follows. In Section 2 we present the properties of the star HD 77407 and the observational techniques. The method of analysis and possible errors in our results are described in Section 3. Finally, a discussion is presented in Section 4, followed by a short section of conclusions.

2 OBSERVATIONS

2.1 The Target Star

The target of our observations, HD 77407, is a slow rotating ($v \sin\ i \simeq 7\,\mathrm{km\ s^{-1}}$) G0V star with a notable chromospheric excess emission in Hα and Ca II triplet line cores. Its distance from the Sun is 30.1 ± 0.8 pc. Its X-ray luminosity exceeds the typical L_{X} of the active Sun by a factor of 30. It is detected as an EUV source and also as radio source with a flux of 1.67 mJy at 20 cm (Wichmann et al. 2003). It is reported to have a large $\mathrm{EW_{Li}}$, indicating it is very young (Montes et al. 2001; Wichmann et al. 2003).

2.2 The Xinglong Data

High-resolution spectra were obtained between January 2004 and May 2006 at the National Astronomical Observatories (Xinglong, China) with the Coudé Echelle Spectrograph and a 1024×1024 Tek CCD attached to the 2.16 m telescope, giving a resolution of the order of 40 000. The exposure times were chosen so as to give a signal-to-noise ratio of above 150. Table 1 shows the log of the observations for HD 77407.

The spectra were reduced with standard MIDAS routines for order identification, background subtraction, flat-fielding correction and extraction of echelle orders and wavelength calibration. Figure 1 shows a portion of the spectrum of HD 77407 around 6712 Å.

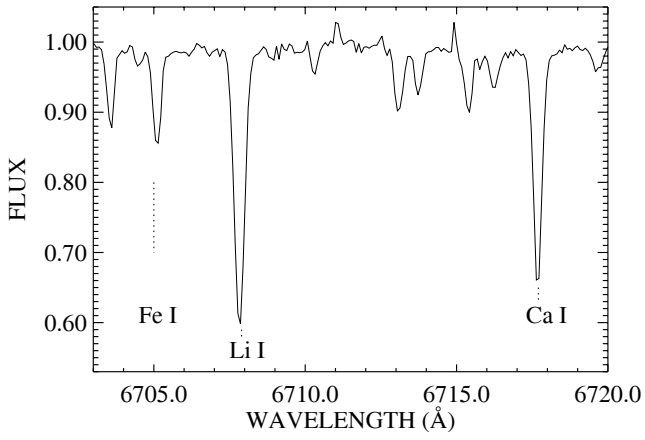

Fig. 1 Li I 6707.8Å and Ca I 6718Å lines for HD 77407.

Table 1 Observational Log for HD 77407

Date	Year	RV (km s^{-1})
Jan. 6	2004	5.0 ± 1.0
Jan. 7	2004	5.0 ± 1.0
Jan. 8	2004	4.3 ± 1.0
Jan. 23	2005	4.1 ± 1.0
May 10	2006	4.4 ± 1.0

Table 2 Comparison of Temperatures from Different Color Index

	$b-y$	$B-V$	$V-K$	$J-H$	$J-K$
Index	0.388	0.60	1.615	0.267	0.360
T (K)	5773	5838	5576	5938	5723

3 ANALYSIS

3.1 Model Atmospheres

Our analyses are based on the line-blanketed local thermodynamic equilibrium (LTE) model atmospheres generated and discussed by Fuhrmann et al. (1997). The main characteristics are: the iron opacity was calculated with the improved meteoritic value $\log\ \varepsilon_{\rm Fe}$=7.51; opacities due to α-elements (O, Ne, Mg, Si, S, Ar, Ca and Ti) for metal-poor stars ([Fe/H] < -0.6) were calculated with the α-element abundances enhanced by 0.4 dex; the mixing-length parameter $l/{\rm H}_p$ was adopted to be 0.5.

3.2 Stellar Parameters

The temperature of HD 77407 has been determined by Marsakov & Shevelev (1995) and Nordstrom et al. (2004) using the color index, however, the difference is very large, the former gave $T_{\rm eff}$ =6049 K, and the later, 5768 K, nearly 300 K lower. Using the calibrations of Alonso et al. (1996) with the Strögren indices from Nordstrom et al. (2004) and $B-V$ color from SIMBAD, we find $T_{\rm eff}(b-y)$=5773 K and $T_{\rm eff}(B-V)$=5838 K, assuming solar metallicity in both cases. Other temperature indicators, such as $V-K$, $J-H$ and $J-K$ indexes, give $T_{\rm eff}$ =5576, 5938 and 5723 K, respectively. Here, the J, H and K values are taken from the 2MASS database. The uncertainties are around 120–140 K for all the determinations. It is noted that the $J-H$ index leads to a temperature much higher than the other indexes. The colour indices as well as the corresponding effective temperatures are summarised in Table 2. Santos et al. (2004) have already noted that the calibration of Alonso et al. (1996) yields systematically lower $T_{\rm eff}$ values by about 139 K than the spectroscopic one, and a similar result was also found by Takeda et al. (2005). Alternatively, slightly higher temperatures can be gotten ($T_{\rm eff}(B-V)$=5883 K and $T_{\rm eff}(b-y)$=5843 K) using the effective temperature scale from Ramírez & Melédez (2005).

Using photometric indices to derive effective temperature is a classical technique commonly used to analyse inactive stars. In the present work, however, we are considering a star with a high level of magnetic activity, which can produce large photospheric spots. Their high activity level could thus affect their spectral energy distribution and therefore their colour indices. Also, Alonso et al.'s (1996) calibrations have been derived for single stars so their validity is established only for single stars. A binary system, in which both components contribute significantly to the total flux, and at the same time differ in colours, will deviate from the colour temperature relation.

In our work, the effective temperature is alternatively derived by fitting the wing of the H $_\alpha$ line profile (Fuhrmann et al. 1993, 1994) [1]. This fitting is shown in Figure 2. We do not apply the broadening theory recently published by Barklem et al. (2000), because it can not reproduce the solar temperature to within 100 K. In addition, it fails to reproduce the profile shape of the higher Balmer lines (H $_\beta$ and up) of stars like HD 140283 and HD 19445 (Korn et al. 2003). Instead we use the resonance broadening as described by Ali & Griem (1965, 1966).

[1] We note that the profile of the H_α line cannot be well fitted, because its core and inner wing are most probably influenced by the chromospheric temperature rise (Barklem 2007).

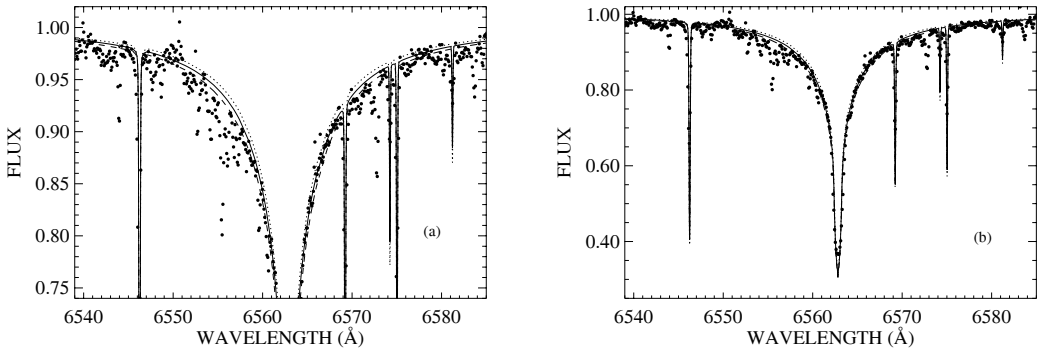

Fig. 2 Profile fits to H_α line in the Xinglong spectrum of HD 77407. The solid line represents the best fit with $T_{\rm eff}$ = 5900 K, while the doted and dashed lines represent $T_{\rm eff}$ = 5820 and 5980 K, respectively. The fitting for the line wing and the whole line is shown in (a) and (b), respectively.

As HD 77407 is an active star, it is doubtful whether the Balmer lines can be reliable tracers of the effective temperature. For instance, Labonte (1986) showed that solar plages affect not only the H_α line cores, but also to a noticeable degree ($\sim$ 0.01) line wings, giving a "lower" effective temperature. It is worth noting that as the H_β line cores are weakly affected by the chromosphere, H_β can probably provide a more reliable effective temperature. Fuhrmann (2004) found, interestingly, that $T_{\rm eff}$, (H_α) and $T_{\rm eff}$ (H_β) are very consistent, implying that the line wings of H_α are not chromospherically affected as are the line cores. This result is also consistent with the finding by Cayrel et al. (1988).

HD 77407 has Hipparcos parallax (ESA 1997), therefore we can calculate the surface gravity $\log\ g$ with the help of

$$\log\ g\ =\ \log\frac{M}{M_\odot} + 4 \times \log\frac{T_{\rm eff}}{T_\odot} + 0.4 \times (M_{\rm bol} - M_{\rm bol_\odot}) + \log\ g_\odot\,.$$

The determination of stellar luminosity requires information of the visual magnitude, interstellar extinction (which is negligible for HD 77407), bolo-metric correction (BC) as tabulated by Alonso et al. (1995), and parallax. The resulting value of $\log\ g$ also depends on the stellar mass. The mass has been estimated from the evolutionary tracks of the α-enhanced stellar models calculated by VandenBerg et al. (2000), with interpolation of abundances. Combining the uncertainties of mass, bolo-metric correction and temperature, the estimate error of $\log\ g$ is less than 0.10.

The iron abundance [Fe/H] is determined by fitting the Fe II lines, as they are not sensitive to NLTE effects, and the microturbulence velocity which is more sensitive to strong lines, is estimated by requiring that the iron abundance derived from Fe II lines should not depend on the equivalent width. A typical error of the microturbulence parameter is about 0.1 km s^{-1}. Finally, the stellar parameters adopted for HD 77407 are: $T_{\rm eff}$ = 5900 K, $\log\ g$ = 4.47, [Fe/H] = 0.07 and ξ = 1.3 km s^{-1}. The expected uncertainty of our temperature is less than 80 K. Though not perfect, our effective temperature is satisfactorily consistent with the value estimated from the calibration of Ramírez & Melédez (2005). The iron abundance is slightly higher than that from Nordstrom et al. (2004).

3.3 Atomic Line Data

Collisional broadening through van der Waals interaction with hydrogen atoms is important for strong lines. The usual procedure is to calculate the C_6 constants from Unsöld's approximation corrected by an empirically enhancement factor, which is adjusted to make the abundances derived from the strong and weak lines agree with each other. Based on a considerably improved atomic theory, O'Mara and his collaborators have published the damping constants for many neutral transitions (Anstee & O'Mara 1995; Barklem & O'Mara 1998; Barklem et al. 1998). Here, we adopt their results, although the actual precision of the calculation is

still under debate (Leininger et al. 2000). As a few lines are too broad when their C_6 values are adopted, we have to decrease C_6 values by 0.2 dex in order to fit these lines better; this is indicated in Table 3. Comparisons with the other computations have been presented by the other authors (Gehren et al. 2001; Mashonkina et al. 2007).

Many of the lines used in this analysis do not have published accurate oscillator strength values. So adjusted values are taken using a theoretical solar model atmosphere with $T_{\rm eff}$ = 5780 K, $\log\ g$ =4.44 and microturbulence ξ = 0.85 km s^{-1}. The result is shown in Table 3.

3.4 The Abundance Determination

The abundance determination is made by using the spectral synthesis method. The synthetic spectra are convolved with the rotational and instrumental broadening profiles, and macroturbulence to match the observed spectral lines (Shi et al. 2002).

The individual derived abundances are also listed in Table 3, and the abundance ratio as a function of the atomic number is shown in Figure 3. The errors quoted in the table are the rms mean abundance based on a sufficient number of lines. Other errors are introduced by uncertainties in the atmospheric parameters. Given the uncertainties in $T_{\rm eff}$, $\log\ g$ and ξ, we estimate an additional error of 0.05 dex, to be added quadratically to the rms errors. Another error source is due to NLTE effects, which are known to affect a few elements, like oxygen, aluminium, potassium, Fe I and, to a lesser extent, carbon, sodium, magnesium, silicon, calcium, Fe II and barium. For the remaining elements, the effects are unknown or uncertain (Zhao et al. 2006).

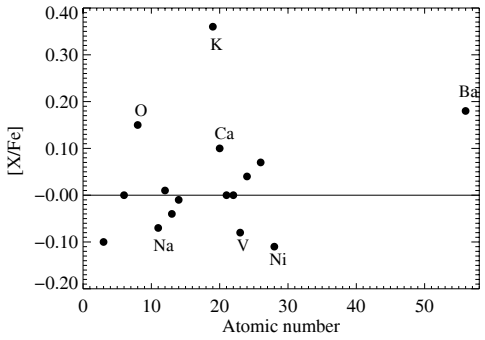

Fig. 3 The abundance ratios derived by us as a function of the atomic number.

3.5 Notes on Individual Abundances

We now discuss the determination of the abundances of individual element and the error estimates.

3.5.1 Oxygen

As the third most abundant element in the Universe, oxygen plays a crucial role in many areas of contemporary astrophysics. The most commonly used permitted O I lines are the triple 7770 Å. It has long been suspected that these lines are not formed in LTE. In the Sun, the NLTE corrections are approximately –0.2 dex (Asplund et al. 2004), or about –0.1 dex if inelastic H collisions (according to Drawin 1968) are adopted (Takeda & Honda 2005). [O/Fe] is about solar for HD 77407 when the NLTE effects are included in our calculation.

3.5.2 α-elements

In active stars, the α-elements, such as magnesium, silicon, calcium and titanium, are often enhanced with respect to iron (e.g. Morel et al. 2003). Excluding [Ca/Fe], we find that [Mg/Fe], [Si/Fe] and [Ti/Fe] for HD 77407 are nearly solar. Katz et al. (2003) also found no α- enhancement for their two active binaries.

Table 3 Atomic Line Data and Derived Abundances (We have decreased the C_6 values by 0.2 dex for the lines marked with asterisks)

λ Å	χ eV	$\log gf$	$\log C_6$	[Fe/H]
Fe I log ($\varepsilon_\odot$)=7.51				
5731.772	4.26	–1.06	–30.683	0.07
5753.132	4.26	–0.65	–30.659	–0.02
5775.088	4.22	–1.08	–30.683	0.04
5806.732	4.61	–0.84	–30.362	0.05
5809.224	3.88	–1.62	–30.388	0.07
5852.228	4.55	–1.19	–30.463	0.05
5856.096	4.29	–1.54	–31.326	0.03
5859.596	4.55	–0.50	–30.583	0.05
5905.680	4.65	–0.73	–30.352	0.01
5916.257	2.45	–2.88	–31.505	0.15
5927.797	4.65	–1.06	–30.363	0.02
5929.682	4.55	–1.19	–30.503	0.04
5930.191	4.65	–0.20	–30.365	0.07
5934.665	3.93	–1.09	–30.384	0.07
5952.726	3.98	–1.34	–30.342	0.01
6003.022	3.88	–1.00	–30.455	0.05
6024.068	4.55	0.03	–30.556	0.06
6027.059	4.07	–1.13	–30.601	0.00
6056.013	4.73	–0.41	–30.315	0.05
6065.494	2.61	–1.50	–31.464	0.01
6079.016	4.65	–0.98	–30.435	0.07
6093.649	4.61	–1.35	–30.500	–0.04
6096.671	3.98	–1.80	–30.381	–0.01
6136.624	2.45	–1.35	–31.526	0.01
6137.702	2.59	–1.35	–31.477	0.07
6151.623	2.18	–3.31	–31.736	–0.03
6157.733	4.07	–1.21	–30.637	0.05
6165.363	4.14	–1.50	–30.583	0.04
6173.341	2.22	–2.86	–31.721	0.09
6180.209	2.73	–2.67	–31.528	0.12
6187.995	3.94	–1.64	–30.449	0.02
6191.571*	2.43	–1.44	–31.739	0.07
6200.321	2.61	–2.35	–31.477	0.03
6219.287	2.20	–2.43	–31.732	0.07
6229.232	2.84	–2.96	–31.480	0.07
6232.648	3.65	–1.24	–30.520	0.10
6240.653	2.22	–3.30	–31.648	0.08
6246.327	3.60	–0.77	–30.554	0.10
6252.565	2.40	–1.64	–31.556	0.02
6265.141	2.18	–2.52	–31.748	0.07
6270.231	2.86	–2.60	–31.479	0.02
6297.799	2.22	–2.73	–31.732	0.07
6322.694	2.59	–2.33	–31.492	0.00
6330.852	4.73	–1.16	–30.441	0.04
6393.612	2.43	–1.49	–31.556	0.05
6411.658	3.65	–0.62	–30.554	0.08
6419.956	4.73	–0.25	–30.477	0.07
6494.994*	2.40	–1.23	–31.772	0.07
6498.945	0.96	–4.66	–31.955	0.02
6518.373	2.83	–2.54	–31.525	0.07
6593.884*	2.43	–2.31	–31.772	0.02
6609.118	2.56	–2.59	–31.526	0.05
6677.997	2.69	–1.35	–31.603	0.09
6703.576	2.76	–3.05	–31.579	0.07
6726.673	4.61	–1.02	–30.472	0.03
6750.164	2.42	–2.56	–31.526	0.09
6752.716	4.64	–1.23	–30.617	0.09
6806.856	2.73	–3.13	–31.603	0.05
6810.267	4.61	–0.98	–30.492	0.07
6828.596	4.64	–0.83	–30.617	0.07
6839.835	2.56	–3.36	–31.542	0.07
6841.341	4.61	–0.67	–30.642	0.14
6842.689	4.64	–1.14	–30.463	0.07
6843.655	4.55	–0.82	–30.666	0.04
6855.166	4.56	–0.60	–30.645	0.07
6858.155	4.61	–0.96	–30.624	0.04
6945.210	2.42	–2.49	–31.539	0.07
6999.885	4.10	–1.37	–30.522	0.04
7022.957	4.19	–1.108	–30.439	0.02
7038.220	4.22	–1.165	–30.414	0.07
7090.390	4.23	–1.082	–30.413	0.04
7130.925	4.22	–0.689	–30.436	0.13
7284.842*	4.14	–1.618	–30.877	0.07
7306.570	4.18	–1.561	–30.520	–0.06
7443.026	4.19	–1.707	–30.423	0.11
7511.031	4.18	0.020	–30.350	0.13
7583.796	3.02	–1.882	–31.425	0.11
7723.210	2.28	–3.460	–31.632	0.07
7748.284	2.95	–1.650	–31.460	0.00
				[Fe/H]$_{\rm I}$=0.05$\pm$0.04
Fe II				
5991.378	3.15	–3.560	–32.190	0.06
6084.110	3.19	–3.820	–32.190	0.04
6247.560	3.87	–2.320	–32.180	0.06
6369.463	2.88	–4.170	–32.110	0.15
6416.928	3.87	–2.550	–32.180	0.05
6432.683	2.88	–3.590	–32.110	0.06
6456.383	3.89	–2.080	–32.180	0.04
6516.083	2.88	–3.280	–32.110	0.10
				[Fe/H]$_{\rm II}$=0.07$\pm$ 0.04
Li I				
6707.760	0.00	0.002	–31.466	–0.10
6707.910	0.00	–0.299	–31.466	–0.10
				[Li/Fe]=-0.10
C I				
6587.61	8.54	–1.15	–29.67	0.00
7113.48	8.65	–0.85	–29.67	0.04
8335.15	7.68	–0.38	–30.73	–0.05
				[C/Fe]= 0.00
O I				
7771.954	9.14	0.43	–31.189	0.15
7774.177	9.14	0.26	–31.189	0.15
7775.395	9.14	0.01	–31.189	0.15
				[O/Fe]=0.15
Na I				
5889.959	0.00	0.110	–31.60	–0.06
5895.932	0.00	–0.190	–31.60	–0.06
6154.228	2.10	–1.570	–30.05	–0.09
6160.751	2.10	–1.280	–30.05	–0.10
8183.260	2.10	0.280	–30.73	–0.06
8194.800	2.10	0.490	–30.73	–0.05
				[Na/Fe]=–0.07 $\pm$ 0.02
Mg I				
7657.603	5.11	–1.268	–29.593	0.02
8806.757	4.35	–0.134	–31.030	0.00
				[Mg/Fe]=0.01 $\pm$ 0.01
Al I				
6696.026	3.14	–1.480	–30.600	–0.10
7835.307	4.02	–0.640	–29.400	–0.13
7836.128	4.02	–0.450	–29.400	–0.10
				[Al/Fe]=–0.11 $\pm$0.01

Table 3 (Continued)

λ Å	χ eV	log gf	log C_6	[X/Fe]
Si I				
5948.540	5.08	–1.110	–29.895	–0.05
6125.021	5.62	–1.500	–29.869	0.02
6142.494	5.62	–1.460	–29.869	–0.03
6145.020	5.62	–1.370	–29.869	–0.07
6237.325	5.62	–1.020	–29.869	0.01
6243.820	5.62	–1.220	–29.868	0.01
6244.474	5.62	–1.240	–29.868	–0.04
6741.634	5.96	–1.540	–29.304	–0.02
6976.513	5.96	–0.980	–29.895	0.00
7003.575	5.96	–0.740	–29.434	–0.04
7005.888	5.96	–0.560	–29.090	0.00
7034.907	5.87	–0.780	–29.027	–0.05
7405.790	5.62	–0.620	–29.869	–0.03
7415.958	5.62	–0.650	–29.969	–0.02
7680.265	5.86	–0.540	–29.485	0.00
7800.003	6.19	–0.680	–28.407	0.05
7849.972	6.19	–0.690	–28.444	–0.05
7932.348	5.96	–0.310	–29.562	–0.04
7943.998	5.96	–0.200	–29.399	0.00
7970.304	5.96	–1.300	–29.550	–0.02
8595.968	6.19	–0.810	–29.039	–0.02
8728.015	6.19	–0.350	–29.347	0.00
8742.458	5.87	–0.360	–30.916	–0.03
8752.014	5.87	–0.190	–30.526	0.00
				[Si/Fe]=–0.01 ± 0.03
K I				
7698.977	0.00	–0.160	–31.121	0.36
				[K/Fe]=0.36
Ca I				
6161.295	2.52	–1.293	–30.364	0.05
6166.440	2.52	–1.186	–30.466	0.00
6169.044	2.52	–0.804	–30.466	0.06
6169.564	2.52	–0.520	–30.464	0.06
6439.083	2.52	0.204	–31.429	0.15
6449.820*	2.52	–0.490	–31.632	0.15
6455.605*	2.52	–1.367	–31.632	0.15
6471.668*	2.52	–0.683	–31.632	0.15
6493.788	2.52	–0.100	–31.580	0.10
6499.654	2.52	–0.769	–31.580	0.10
6717.687	2.71	–0.450	–30.348	0.08
				[Ca/Fe]=0.10 ± 0.05
Sc II				
6604.600	1.36	–1.080	–32.137	0.00
				[Sc/Fe]=0.00
Ti I				
5866.461	1.07	–0.813	–31.809	0.00
5953.170	1.89	–0.350	–31.807	0.00
6258.110	1.44	–0.394	–31.461	–0.01
				[Ti/Fe]= 0.00
V I				
5727.057	1.08	0.090	–31.498	–0.08
6090.216	1.08	–0.081	–31.537	–0.08
				[V/Fe]=–0.08
Cr I				
5783.866	3.32	–0.250	–30.246	0.03
5787.926	3.32	–0.070	–30.247	0.04
6979.806	3.46	–0.254	–30.529	0.04
7355.891	2.89	–0.190	–30.450	0.03
				[Cr/Fe]= 0.04
Ni I				
5754.666	1.93	–1.852	–31.562	–0.18
5805.226	4.17	–0.510	–30.534	–0.05
6086.288	4.26	–0.370	–30.536	–0.17
6108.125	1.68	–2.388	–31.752	–0.20
6111.078	4.09	–0.753	–30.529	–0.10
6130.141	4.26	–0.883	–30.555	–0.10
6176.816	4.09	–0.152	–30.554	–0.10
6327.604	1.68	–3.000	–31.780	–0.06
6482.809	1.93	–2.708	–31.677	–0.12
6586.319	1.95	–2.688	–31.684	–0.15
6772.321	3.66	–0.908	–30.588	–0.04
7110.905	1.93	–2.884	–31.755	–0.13
7122.206	3.54	–0.119	–30.588	–0.10
7414.514	1.99	–2.10	–31.765	–0.14
7422.286	3.63	–0.20	–30.581	–0.10
7727.616*	3.68	–0.18	–30.805	–0.08
				[Ni/Fe]=–0.11 ± 0.05
Ba II				
5853.688	0.60	–0.820	–1.850	0.15
6496.908	0.60	–0.127	–31.890	0.20
				[Ba/Fe]=0.18

The NLTE effects for Mg, Si and Ca are negligible for our target star (Zhao & Gehren 2000; Shi et al. 2007, in preparation; Mashonkina et al. 2007) .

3.5.3 Sodium, Aluminium and Potassium

[Na/Fe] is under solar. The NLTE effects for Na are negative and not important for solar-type stars (Shi et al. 2004). Analyses adopting the LTE assumption for Al and K are often widely misleading (Asplund 2005), because the NLTE effects for aluminium and potassium are large even for solar-type stars (Gehren et al. 2006; Zhang et al. 2006). [Al/Fe] is –0.04 when the NLTE effects are included. The NLTE effect for potassium is about –0.4 dex for solar like stars (Zhang et al. 2006). So, [K/Fe] is about solar for this star when the NLTE effect is considered.

3.5.4 Scandium, Vanadium, Chromium and Nickel

While the scandium and chromium abundances are nearly solar, vanadium and nickel exhibit a modest underabundance. Similar result was found for active binaries by Morel et al. (2003) and Katz et al. (2003). It is noted that the hyperfine splitting effects can be important for Sc II and V I lines, however, they are less

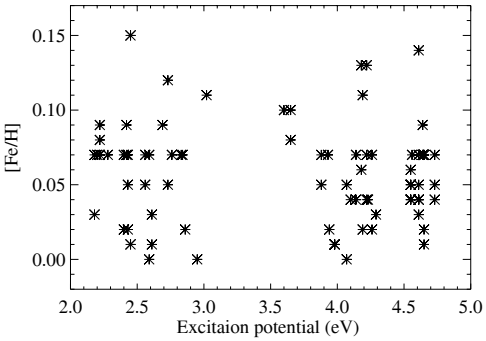

Fig. 4 [Fe/H] as a function of the excitation potential for 79 Fe I lines.

than 0.1 dex for Sc II 6604 Å and V I 5727 Å and 6090 Å lines for solar-type stars (Prochaska & MacWilliam 2000; Chen et al. 2000). Blackwell et al. (1987) have shown the presence of a 0.098 dex deviation for low excitation lines in the solar Cr I spectrum, and suggested it is due to the NLTE effects. It is expected that the NLTE effects are not important for Cr I lines in HD 77407.

3.5.5 Fe I

We used 79 Fe I lines to determine the $[\mathrm{Fe/H}]_{\mathrm{I}}$ abundances, and the $[\mathrm{Fe/H}]_{\mathrm{I}}$ versus excitation potential is plotted in Figure 4. It shows that there is not any trend between the Fe I abundances and excitation potential, which suggests that the temperature determined from H_{α} line wings is appropriate. The mean $[\mathrm{Fe/H}]_{\mathrm{I}}$ is 0.05 ± 0.04. So the difference for the iron abundance from Fe I and Fe II is 0.02, which indicates that the precision of our T_{eff} and $\log\ g$ is realistic. The NLTE effects for Fe I lines are negligible for our target star (Korn et al. 2003).

3.5.6 Barium

Overabundance of the s-process element barium has been found. The NLTE effects are negligible for Ba for our target star (Mashonkina et al. 1999).

4 DISCUSSION

4.1 Heliocentric Radial Velocity

The line profile can be used to measure the radial velocity of the star. The observed RV is converted to heliocentric radial velocity using compute/barycorr in MIDAS. For HD 77407 we have acquired five RV measurements at unequal intervals. They are around 4.4 km s $^{-1}$(see Table 1), which is consistent with the result of 4.4 km s^{-1} from the SIMBAD database. Unfortunately, our measurements are not accurate enough for a definite conclusion on whether HD 77407 is a binary. Recently, Mugrauer et al. (2004) found that this star has a low-mass stellar companion using both proper motion measurement and spectroscopy. They took multi-epoch high-resolution spectra of HD77407 to search for sub-stellar companions, but did not find any with $3M_{\mathrm{Jup}}$ upper mass ($m \sin\ i$) limit. However, they detected a long-term radial velocity variation trend for HD77407, which is consistent with a $\sim 0.3\ M_{\odot}$ companion at ~ 50 AU separation.

4.2 Hα and Ca II Activity: the Proxy for Stellar Activity

Hα and Ca II triple lines are often used as a proxy for stellar activity. Thatcher & Robinson (1993) suggested that the Hα line is collisionally filled in as a result of the higher temperatures within the lower layers of the chromosphere. The increased temperature of an active chromosphere has the effect of increasing the electron density at this layer where the Hα is formed. The emission component of the Hα line is determined by subtracting the spectrum of an appropriate inactive star with a similar spectral type (Thatcher & Robinson 1993). A comparison of the Hα and Ca II 8542 Å lines between this star and the normal star HD 167588 with similar spectral type is shown in Figure 5. A noticeable filling-in was detected in the Hα and Ca II IRT lines of HD 77407. During the night of 2005 January 23, a noticeable increase in the excess emission

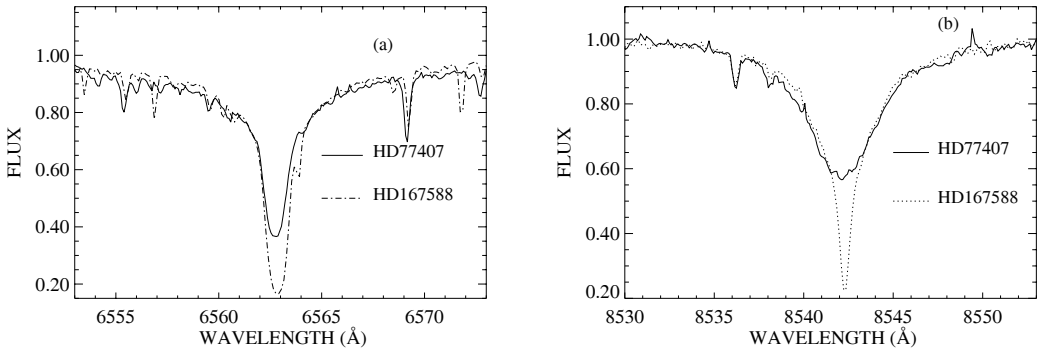

Fig. 5 Spectra of the HD 77407 and HD 167588 around the H_α (a) and Ca II 8542 Å (b) lines. A noticeable filling-in can be seen in the Hα and Ca II lines for HD 77407.

was detected, and the Ca II 8542 Å line showed a strong emission core. This variation could be due to a small-scale flare or to the transit of an active region.

4.3 Lithium 6707.8 Å Line: an Age Indicator

The Li I 6707.8 Å line is often used as an indicator of age for single stars. The line is actually a doublet split by fine structure. The major contribution comes from the more abundant ^{7}Li isotope. Because of blending with weak Fe I, V I lines, care should be taken when fitting the line. The Li lines in the solar spectrum could not be reliably measured, so we are using directly the atomic parameters for the lines. The gf values of the Li lines are among the most accurate of stellar lines (Smith et al. 1998), and can safely be used in an absolute manner. The lithium abundance we derived is A(Li) = 3.20, 3.06 and 3.12 for LTE, NLTE, and NLTE with charge reaction included (Shi et al. 2007). The equivalent width measured is 181.1 m Å, which is in agreement with the previous works (Montes et al. 2001; Wichmann et al. 2003). The Li abundances are slightly lower than the one from the meteorite. This may be due to the pre-main sequence Li depletion as discussed by Xing et al. (2007). Figure 1 shows the strength of the lithium feature, which is compared with the Ca I 6717.7 Å line.

5 CONCLUSIONS

In this paper we have analysed the high-resolution spectra of the active ZAMS star HD 77407. Our main results can be summarized as follows:

1. Our results demonstrate that it is an active star with the H_α and Ca II triple line cores showing emission features.
2. The high lithium 6707.8 Å equivalent width indicates it is a very young star. Although the lithium abundance is high, it is about 0.2 dex lower than the one from the meteorite, which may be due to the pre-main sequence lithium depletion.
3. The abundances for most elements are nearly solar, however, Ca and Ba are enhanced, Na, V, and Ni are underabundant.

Acknowledgements This work is financially supported by the National Natural Science Foundation of China under grants No.10433010 and No.10521001.

References

Ali A. W., Griem H. R., 1965, Phys. Rev., 140, 1044
Ali A. W., Griem H. R., 1966, Phys, Rev., 144, 366
Alonso A., Arribas S., Martinez-Roger C., 1995, A&A, 297, 197
Alonso A., Arribas S., Martinez-Roger C., 1996, A&A, 313, 873

Anstee S. D., OMara B. J., 1995, MNRAS, 276, 859
Asplund M., 2005, ARA&A, 43, 481
Asplund M., Grevesse N., Sauval A. J., Allende Prieto C., Kiselman D., 2004, A&A, 417, 751
Barklem P. S., 2007, A&A, 466, 327
Barklem P. S., O'Mara B. J., 1998, MNRAS, 300, 863
Barklem P. S., O'Mara B. J., Ross J. E., 1998, MNRAS, 296, 1057
Barklem P. S., Piskunov N., O'Mara B. J., 2000, A&A, 363, 1091
Blackwell D. E., Booth A. J., Menon S. L. R., Petford A. D., 1987, A&A, 180, 229
Cayrel R., Cayrel de Strobel G., Dennefeld M., 1988, IAU Symp., 132, 449
Chen Y. Q., Nissen P. E., Zhao G., Zhang H. W., Benon T., 2000, A&AS, 141, 491
Dall T. H., Bruntt H., Strassmeier K. G., 2005, A&A, 444, 573
Drawin H. W., 1968, Z. Physik, 211, 404
ESA1997, The Hipparcos and Tycho Catalogues, ESA, SP-1200
Favata F., Micela G., Sciortino S., Morale F., 1997, A&A, 324, 998
Fuhrmann K., Axer M., Gehren T., 1993, A&A, 271, 369
Fuhrmann K., Axer M., Gehren T., 1994, A&A, 285, 585
Fuhrmann K., Pfeiffer M., Frank C. et al., 1997, A&A, 323, 909
Fuhrmann K., 2004, AN, 325, 3
Gehren T., Butler K., Mashonkina L., Reetz J., Shi J. R., 2001, A&A, 366, 981
Gehren T., Shi J. R., Zhang H. W., Zhao G., Korn A. J., 2006, A&A, 451, 1065
Güdel M., 2004, A&A Rev., 12, 71
Jordan C., Doschek G. A., Drake J. J., Galrin A. B., Raymond J. C., 1998, ASPCS, 154, 91
Katz D., Favata F., Aigrain S., Micela G., 2003, A&A, 397, 747
Korn A. J., Shi J. R., Gehren T., 2003, A&A, 407, 691
Labonte B. J., 1986, ApJS, 62, 241
Leininger T., Gadéa F. X., Dickinson A. S., 2000, J. Phys. B: At. Mol. Opt. Phys., 33, 1805
Mashonkina L., Gehren T., Bikmaev I., 1999, A&A, 343, 519
Mashonkina L., Korn A. J., Przybilla N., 2007, A&A, 461, 261
Marsakov V. A., Shevelev Yu. G., 1995, BICDS, 47, 13
Montes D., López-Santiago J., Fernández-Figueroa M. J., Gálvez M. C., 2001, A&A, 379, 976
Morel T., Micela G., Favata F., Katz D., Pillitteri I., 2003, A&A, 412, 495
Morel T., Micela G., Favata F., Katz D., 2005, A&A, 444, 573
Mugrauer M., Neuhäuser R., Guenther E. W. et al., 2004, A&A, 417, 1031
Nordstrom B., Mayor M., Andersen J. et al., 2004, A&A, 418, 989
Prochaska J. X., McWilliam A., 2000, ApJ, 537, L57
Ramiírez I. Q., Melédez J., 2005, ApJ, 626, 465
Randich S., Gratton R., Pallavicini R., 1993, A&A, 273, 19
Santos N. C., Israelian G., Mayor M., 2004, A&A, 415, 1153
Schlegel D. J., Finkbeiner D. P., Davis M., 1998, ApJ, 500, 525
Shi J. R., Gehren T., Zhang H. W., Zeng J. L., Zhao G., 2007, A&A, 465, 587
Shi J. R., Gehren T., Zhao G., 2004, A&A, 423, 683
Shi J. R., Zhao G., Chen Y. Q., 2002, A&A, 381, 982
Shkolnik E., Walker G. A. H., Bohlender D. A., 2003, ApJ, 597, 1092
Smith V. V., Lambert D. L., Nissen P. E., 1998, ApJ, 506, 405
Soderblom D. R., Stauffer J. R., Hudon J. D., Jones B. F., 1993, ApJS, 85, 315
Takeda Y., Honda S., 2005, PASJ, 57, 65
Takeda Y., Ohkubo M., Sato B., Kambe E., Sadakane K., 2005, PASJ, 57, 27
Thatcher J. D., Robinson R. D., 1993, MNRAS, 262, 1
VandenBerg D. A., Swenson F. J., Rogers F. J. et al., 2000, ApJ, 532, 430
Wichmann R., Schmitt J. H. M. M., Hubrig S., 2003, A&A, 399, 983
Wichmann R., Schmitt J. H. M. M., 2003, MNRAS, 342, 1021
Wielen R., 1977, A&A, 60, 263
Xing L. F., Shi J. R., Wei J. Y., 2007, New Astronomy, 12, 265
Young P. R., 2005, A&A, 439, 361
Zhang H. W., Gehren T., Butler K., Shi J. R., Zhao G., 2006, A&A, 457, 645
Zhao G., Chen Y. Q., Shi J. R. et al., 2006, Chin. J. Astron. Astrophys. (ChJAA), 6, 265
Zhao G., Gehren T., 2000, A&A, 362, 1077